NREL
NATIONAL RENEWABLE ENERGY LABORATORY

Final Report for PV Incubator Subcontract No. NAT-7-77015-05

October 19, 2007 – July 30, 2009

Noren Pan
MicroLink Devices
Niles, Illinois

NREL Technical Monitor: Kaitlyn VanSant

NREL is a national laboratory of the U.S. Department of Energy, Office of Energy Efficiency & Renewable Energy, operated by the Alliance for Sustainable Energy, LLC.

Subcontract Report
NREL/SR-5200-54691
April 2012

Contract No. DE-AC36-08GO28308

NREL
NATIONAL RENEWABLE ENERGY LABORATORY

Final Report for PV Incubator Subcontract No. NAT-7-77015-05

October 19, 2007 – July 30, 2009

Noren Pan
MicroLink Devices
Niles, Illinois

NREL Technical Monitor: Kaitlyn VanSant
Prepared under Subcontract No. NAT-7-77015-05

NREL is a national laboratory of the U.S. Department of Energy, Office of Energy Efficiency & Renewable Energy, operated by the Alliance for Sustainable Energy, LLC.

National Renewable Energy Laboratory
15013 Denver West Parkway
Golden, Colorado 80401
303-275-3000 • www.nrel.gov

Subcontract Report
NREL/SR-5200-54691
April 2012

Contract No. DE-AC36-08GO28308

This publication was reproduced from the best available copy submitted by the subcontractor and received no editorial review at NREL.

NOTICE

This report was prepared as an account of work sponsored by an agency of the United States government. Neither the United States government nor any agency thereof, nor any of their employees, makes any warranty, express or implied, or assumes any legal liability or responsibility for the accuracy, completeness, or usefulness of any information, apparatus, product, or process disclosed, or represents that its use would not infringe privately owned rights. Reference herein to any specific commercial product, process, or service by trade name, trademark, manufacturer, or otherwise does not necessarily constitute or imply its endorsement, recommendation, or favoring by the United States government or any agency thereof. The views and opinions of authors expressed herein do not necessarily state or reflect those of the United States government or any agency thereof.

Available electronically at http://www.osti.gov/bridge

Available for a processing fee to U.S. Department of Energy and its contractors, in paper, from:

U.S. Department of Energy
Office of Scientific and Technical Information
P.O. Box 62
Oak Ridge, TN 37831-0062
phone: 865.576.8401
fax: 865.576.5728
email: mailto:reports@adonis.osti.gov

Available for sale to the public, in paper, from:

U.S. Department of Commerce
National Technical Information Service
5285 Port Royal Road
Springfield, VA 22161
phone: 800.553.6847
fax: 703.605.6900
email: orders@ntis.fedworld.gov
online ordering: http://www.ntis.gov/help/ordermethods.aspx

Cover Photos: (left to right) PIX 16416, PIX 17423, PIX 16560, PIX 17613, PIX 17436, PIX 17721

Printed on paper containing at least 50% wastepaper, including 10% post consumer waste.

Executive Summary

The Solar America Initiative is intended to provide numerous technological routes towards a lower levelized cost of solar-generated electricity (LCOE). MicroLink's planned contribution towards the SAI is to provide a method of lowering the cost of GaAs-based solar cells, which are a major contributor to the cost of concentrator photovoltaic (CPV) modules. MicroLink's unique approach is to use an epitaxial liftoff (ELO) process to completely remove the active solar cell from the substrate while preserving the performance and yield of the cell. The substrate accounts for approximately half the cost of conventional, multi-junction GaAs-based solar cells. By using ELO, the substrate can be reused several times for additional solar cell growths, thereby reducing the cost of multi-junction solar cells by up to 50%.

In terms of technology development, this subcontract has been very successful. All of the technical milestones have been reached on or ahead of schedule. All of the deliverables have been produced on or ahead of schedule and have met or exceeded performance goals.

MicroLink is seeking ways to generate a return on the taxpayer's investment in the ELO technology. The company is developing solar cell products based on ELO and plans to enter the market for solar cells for terrestrial CPV installations in the near future. To this end, MicroLink plans to construct a solar cell manufacturing facility in the Chicago area. To protect the intellectual property generated as a result of the SAI program, MicroLink has filed applications for US patents. PCT applications, which provide the option of worldwide coverage, have also been filed.

This SAI subcontract has provided MicroLink with a clear and solid pathway towards becoming a major supplier of high efficiency GaAs-based solar cells. The key differentiators between MicroLink and other GaAs solar cell suppliers include a lower cost structure and a projected reduction in thermal resistance due to the absence of the semiconductor substrate. A reduction in the thermal resistance is expected to significantly increase the performance of the GaAs based solar cell at high concentration. The achievement of high efficiency has significantly increased the acceptance of MicroLink Devices as a future supplier of high efficiency dual and IMM (inverted metamorphic) solar cells. MicroLink entered the SAI program with a 10% efficiency GaAs solar cell (1-sun AM 1.5) and finished the program with a 30% efficient IMM solar cell. The lightweight aspect of the ELO has also attracted significant interest from other DOD (Department of Defense) for remote and near-space power generation. This work provided employment for five full time engineers who worked on providing the deliverables for this report.

A summary of the subcontract tasks is presented in a Gantt chart in Figure 1.

**Unless otherwise noted, all images in this report are property of MicroLink Devices.*

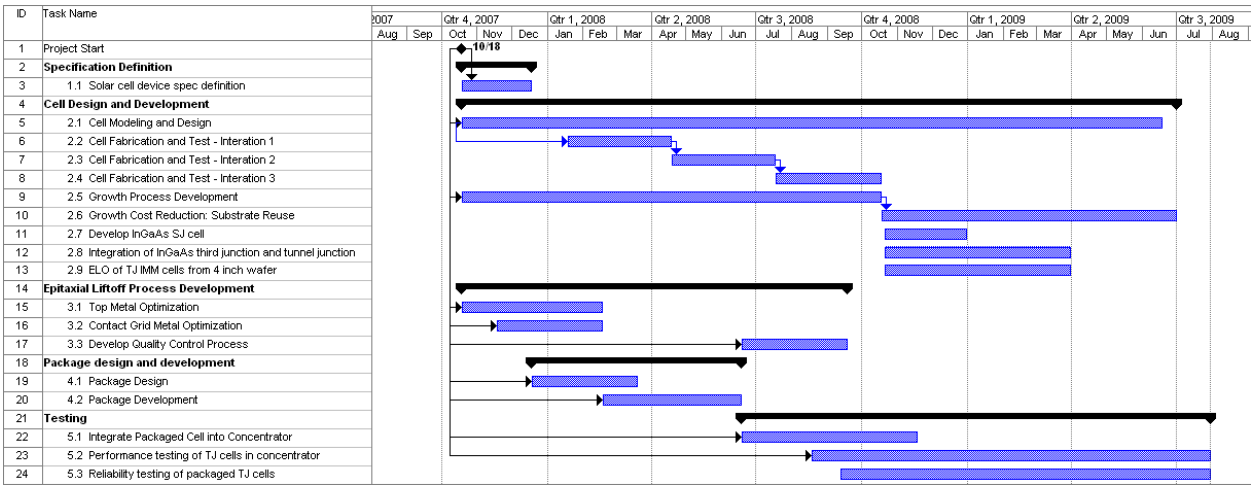

Figure 1: Gantt Chart showing subcontract task structure.

Work Accomplished in Most Recent Quarter

Task 5.2: Performance Testing in Concentrator

Milestone: Complete efficiency test of packaged triple junction cells in concentrator.

Deliverable: Efficiency of packaged triple junction liftoff cell = 25% under at least 500x concentration.

Status: Completed on schedule.

The specific objectives of this work are to develop low-cost, multi-junction solar cells based on an ELO technique. The resulting solar cells are intended for use in concentrator systems at concentration ratios up to 500x. In the past we have demonstrated packaging of ELO cells on a ceramic mount, which can be integrated into concentrator system. In this task, the milestone is to complete efficiency test of packaged triple junction cells under concentration. Alpha-Omega flash tester employed to generate high-concentration AM1.5 illumination is shown in Figure 1.

Figure 2: Photograph of Alpha-Omega flash tester employed to test ELO cells under concentration.

ELO triple-junction cells were mounted on metallized ceramic mounts with conducting paste or soldered using indium. Subsequently, wire bonding from the top of the bus bars onto adjacent bonding pads was done to facilitate probing the cells for current and voltage leads. In Figure 3, a packaged ELO triple-junction cell is shown.

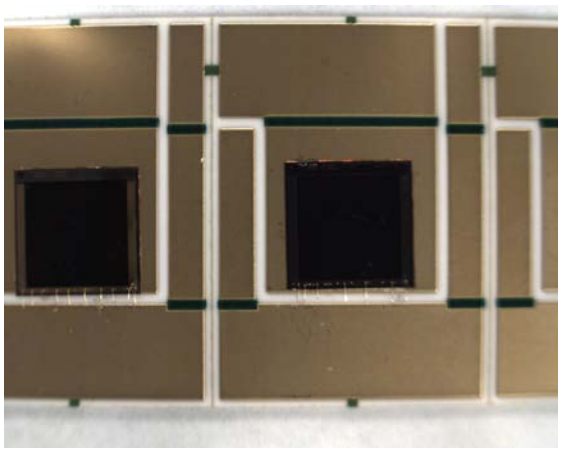

Figure 3: Photograph of packaged triple-junction ELO cell for testing at 500 suns.

In Figure 4 variation of efficiency of packaged ELO triple junction cell as a function of illumination intensity is plotted. It is clear from the Figure that we have achieved efficiencies of 26.8% at 500 suns. This number significantly exceeds the Deliverable #24 requirements.

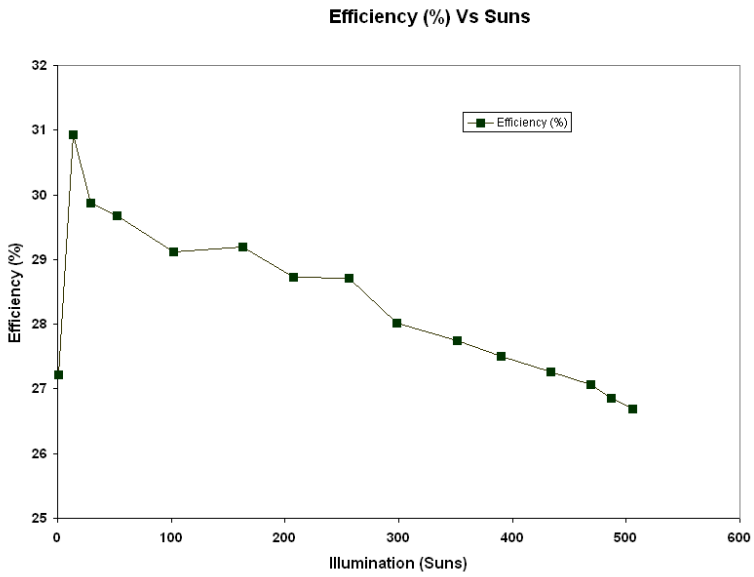

Figure 4: Efficiency of 3J cells as a function of concentration.

It is also clear from Figure 4 that the efficiency of the packaged cells reached a maximum of 31% at about 11 suns. At higher illumination intensities, there is gradual drop in the efficiency, which is attributed to the high series resistance of the cells. We are currently working on reducing the series resistance of the triple-junction cells by redesigning the structure and doping profile. It should be noted that the series resistance is a distributed parameter in solar cells: part of the series resistance comes from the grid metallization and associated resistance. We are also working on developing new designs to optimize the resistance loss in the emitter grid design.

Task 5.3: Reliability Testing

Milestone: Complete initial reliability testing of packaged triple junction solar cell.

Deliverable: Results of tests listed in Attachment 1 and failure analysis if necessary.

Status: Completed on schedule.

The goal of the task is the preliminary evaluation of reliability performance of packaged ELO triple-junction solar cells. Within the scope of this project, it is not possible to completely characterize the reliability performance of the triple-junction ELO cells. In this task, we have therefore decided to use the Thermal Cycling test, as defined in the IEC62108 document, and specified for concentration systems, as the reliability test that is most likely to excite the failure modes expected to be observed in the field. Our results show that the ELO cells, as designed, can withstand the temperature cycling without debonding. The tests also revealed that more comprehensive analysis and performance improvement is needed before these cells deployed in the field.

Experimental Procedure for Thermal Cycling:

Two groups of triple junction solar cells were thermally cycled from –40 °C to 110 °C per IEC62108. Group I devices were electrically biased during part of a thermal cycle; Group II devices were not electrically biased.

Group I devices consisted of five packaged triple junction solar cells. The devices were electrically cycled when the ambient temperature was above 25 °C for a total of 10 on-off cycles. The duty cycle was 50%. The period, T, of electrical cycling was selected so that $T = t/10$, where t is the time that the ambient temperature is above 25 °C during one thermal cycle. Group II consisted of four packaged triple junction solar cells. Group II devices were thermally cycled, only; no electrical bias was applied.

Reliability Results

The five Group I packaged solar cells, biased with a constant current, had one failure due to a lack of adhesion between the solar cell and the substrate. The integrity of the bond between the solar cell and substrate on the remaining four devices did not appear to degrade after 500 thermal cycles. On the other hand, the four remaining solar cells electrically shorted prior to the first read point at 25 thermal cycles. Since the devices failed early in the test, sufficient time was available to produce a second set of packaged solar cells: Group II. Group II devices were not electrically biased during thermally cycling. All four Group II devices showed various degrees of performance degradation in efficiency, fill factor, V_{oc}, and I_{sc}. Three of the four devices are still functional at 460 cycles. For the Group II devices the degradation in performance is believed to be due, at least partially, to the degradation of the antireflection coating.

Four of the five Group I packaged solar cells survived 500 thermal cycles without the solar cell delaminating from the substrate. The one device in which the adhesion was lost between solar cell and the substrate failed during the first 25 cycles. Since this device was one of the first produced, its failure was attributed to operator error.

Group II packaged solar cells were not electrically cycled during thermal cycling. These devices provided quantitative performance data for the solar cell package. Of the four packaged solar cells, only Device 3 showed a significant degradation. The root cause for Device 3's large decrease in Voc is still under investigation. One possible root cause is an electrical short in the package.

One possible root cause of the performance decrease in Devices 1, 2, and 4 is degradation of the antireflection coating. The variation in antireflection coating degradation could explain at least part of the decrease in performance, if not all of it. In addition, coating degradation was first observed at the 25 thermal cycle read point. Thus, the performance degradation is consistent with the coating degradation. Additional testing is required to verify that the antireflection is indeed responsible for the performance degradation in Devices 1, 2, and 4.

Summary of Work Accomplished During the Program

A summary of the deliverables associated with this program and MicroLink's performance relative to schedule is shown in Table 1. MicroLink is pleased to note that all deliverables have been provided on or ahead of schedule. All technical performance parameters have been met or exceeded.

Table 1: Summary of program deliverables

No.	Title	Due	Delivered	Status	Technical Goals
1.	Solar Cell Device Specification	12/18/07	12/17/07	On time	Achieved
2.	Quarterly Report #1	02/02/08	01/25/08	On time	
3.	Growth Process Development: Junction QE Targets	02/18/08	02/15/08	On time	Achieved
4.	Top Metal Optimization	02/18/08	02/15/08	On time	Achieved
5.	Contact Grid Metal Optimization	02/18/08	02/15/08	On time	Achieved
6.	Cell Fabrication and Test Iteration 1	04/18/08	04/16/08	On time	Achieved
7.	Quarterly Report #2	05/02/08	04/18/08	On time	
8.	Growth Process Development Cell Fill Factor Targets	06/18/08	04/17/08	8 wks early	Achieved
9.	Package Development	06/18/08	06/17/08	On time	Achieved
10.	Cell Fabrication and Test Iteration 2	07/18/08	07/16/08	On time	Achieved
11.	Stage Gate	07/18/08	07/18/08	On time	
12.	QC Process Development	09/18/08	07/17/08	9 wks early	Achieved
13.	5.1 Integrate Packaged Cell into Concentrator	11/30/08	11/30/08	On time	Achieved
14.	2.4 Cell Fabrication and Test Iteration 3	12/30/08	10/28/08	8 wks early	Surpassed
15.	2.5 Growth Process Development: Process for Fabricating ELO Cells	10/28/08	10/28/08	On time	Achieved
16.	2.7 InGaAs Third Cell Development	12/30/08	12/29/08	On time	Achieved
17.	Quarterly Report #3	12/30/08	12/29/08	On time	
18.	2.6 Growth Cost Reduction: Substrate Reuse: 1x Reuse of Wafer	02/28/09	02/26/09	On time	Achieved
19.	2.8 Inverted Triple Junction Optimization	03/30/09	03/30/09	On time	Achieved
20.	2.9 ELO of Triple Junction Cell	03/30/09	03/30/09	On time	Achieved
21.	Quarterly Report #4	03/30/09	03/30/09	On time	
22.	2.6 Growth Cost Reduction: Substrate Reuse: 2x Reuse of Wafer	04/30/09	04/30/09	On time	Achieved
23.	2.6 Growth Cost Reduction: Substrate Reuse: Significant Cost Reduction	06/30/09	06/30/09	On time	Achieved
24.	5.2 Performance Testing in Concentrator	07/30/09	07/30/09	On time	Surpassed
25.	5.3 Reliability Testing	07/30/09	07/30/09	On time	Achieved
26.	Final Report	07/30/09	07/30/09	On time	

1.1 Solar Cell Device Specification

Milestone: Solar cell specification complete

Deliverable: Specification for solar cell agreed between MicroLink Devices and subcontractor. Specification to contain definition of mechanical, electrical, and optical properties.

Status: Completed on schedule.

Specifications for a solar cell that would be useable in a practical concentrator were developed in consultation with our subcontractor. The mechanical dimensions of the solar cell die were fixed and active area of 10 mm x 10 mm was adopted. A set of four metal grid designs was specified and engineering drawings of the solar cell design were produced.

The layout of the solar cell is shown in Figure 5.

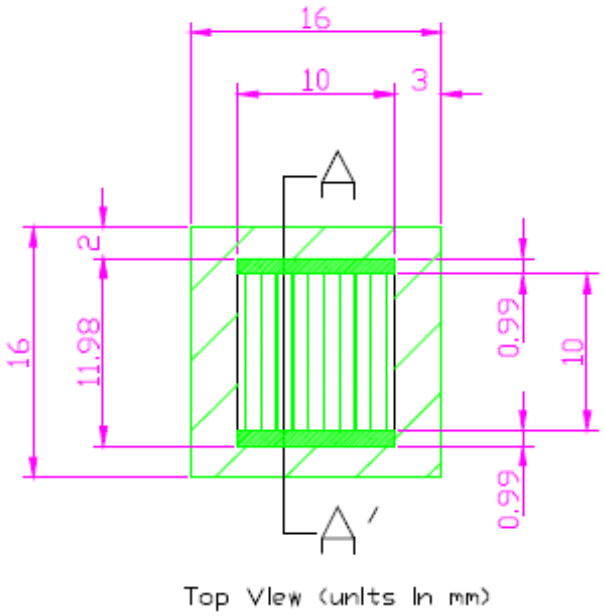

Figure 5: Layout of the solar cell.

2.1 Cell Modeling and Design

Milestone: None.

Deliverable: Tied to deliverables for tasks 2.2, 2.3, 2.4, and tasks 2.7 through 2.9.

Status: No separate submissions for this task.

The overall goal of this task was the construction of an electrical, optical, and thermal model of multi-junction solar cells. The model was implemented in the Synopsys TCAD simulator suite for heterostructure designs developed by MicroLink. Material parameters were extracted from the literature and from MicroLink-grown material. The predictions of the model were compared with the results of cell test and the model was modified and refined as necessary. The model

includes electrode contact layouts and illumination of the heterostructure by an AM1.5 spectrum. The model is capable of handling light concentrations up to several hundred. The model includes a two-layer antireflection coating on the as-grown structure.

The model was used to assist with the cell fabrication and test tasks. Specifically, the model was used to calculate optimal sub-cell thicknesses in order to maximize the current density of the dual- and triple-junction cells. Studies were performed to determine good designs for contact metal compositions, thicknesses, and layouts. Good results were obtained in a number of areas:

1. Antireflection Coating Model Development and Dual-Junction Cell Simulation

The ARC coating designs considered were based on a two-layer stack. This material combination was chosen to be consistent with MicroLink's fabrication capabilities. The procedure used to optimize the ARC consists of calculating the current density generated in a dual-junction solar cell under AM1.5 illumination. This current density calculation is performed for a coarse mesh of stack layer thicknesses in order to identify promising thickness regimes, and is followed by an optimization over a finer mesh in order to maximize the current in the dual-junction cell.

Performing a fine mesh optimization centered on the peak cell currents identified in the coarse mesh simulations worked well. This procedure resulted in a dual-junction cell current under AM1.5 illumination that is 38% higher than that of an uncoated cell, and is appreciably better than the solution found in the coarse mesh optimization step. The sensitivity of the current density to stack layer thicknesses suggested that the designed ARC is achievable with typical evaporated film fabrication process tolerances without the use of in-situ reflectance monitoring. A similar approach was used in triple-junction cells.

2. Optimization of Cell Design

We developed a procedure for optimizing the overall cell design, i.e., optimizing the sub-cell thicknesses and the ARC stack layer thicknesses simultaneously in order to reach a global efficiency maximum. In the case of a dual-junction cell, the overall procedure consisted of adjusting the sub-cell thicknesses to match their currents. This was done with a constant dual-layer antireflection coating optimized for the baseline structure. Once the sub-cell thicknesses had been optimized, the antireflection coating stack layer thicknesses were optimized to maximize the cell current. We found that the total cell current improved by ~6% compared to the baseline design. A similar approach was used in triple-junction cells.

3. Temperature Dependence of Cell Performance

Simulations of ELO cell temperatures at illuminations up to 500x were performed. The results of these simulations were compared with the results of simulations of an identical cell structure on a thick GaAs substrate and on a Ge substrate. A non-isothermal hydrodynamic simulation framework was used to simulate dual-junction cells based on a MicroLink structure. An AM1.5 spectrum with concentration up to 500x was used for this evaluation.

The illumination concentration dependence of the cell temperature was also simulated. This simulation showed that the ELO structure results in a considerably reduced maximum temperature rise compared with GaAs and Ge substrates under all illumination conditions. This has significant implications for ultimate cell efficiency.

4. Cell Performance vs. Illumination Intensity

The impact of the concentration ratio on cell efficiency performance was evaluated. The simulated current-voltage characteristics as a function of substrate type (ELO, Ge, and GaAs) and illumination intensity were analyzed using scripts written in Matlab. For this analysis, several limiting cases were examined. To assess the intrinsic limitations of the cells, the performance of cells with ideal ohmic contacts was determined, followed by an evaluation of the impact of several levels of specific contact resistance for the top grid metallization. ELO provided a negligible advantage at lower concentrations, but a significant effect for concentrations exceeding approximately 100. To assess the impact of realistic contact resistances on cell performance, the intrinsic current-voltage characteristics obtained from the non-isothermal simulations were post-processed to include finite contact resistances. Contact resistance has a very minor effect under low illumination intensity and, as expected, progressively becomes more significant as the illumination intensity is increased.

2.2 Cell Fabrication and Test Iteration 1

Milestone: Fabrication and test of solar cell.

Deliverable: Dual-junction cell with efficiency 22% under 1 sun AM1.5 illumination.

Status: Submitted on schedule.

The IV curve of a cell fabricated as part of this task and measured at NREL is shown in Figure 6. The measured efficiency was 22.05%, which slightly exceeded the target value. In order to achieve this goal we analyzed the performances of both the top and bottom cells individually in an upright structure (on a thick substrate) and also in the ELO form. The ELO GaAs single junction solar cells were found to exhibit inferior performance when compared to those fabricated on a thick substrate. This problem was solved by adjusting growth temperature profiles and dopant values. This resulted in a dramatic improvement of the efficiency of our dual-junction cells from <15% to >22%.

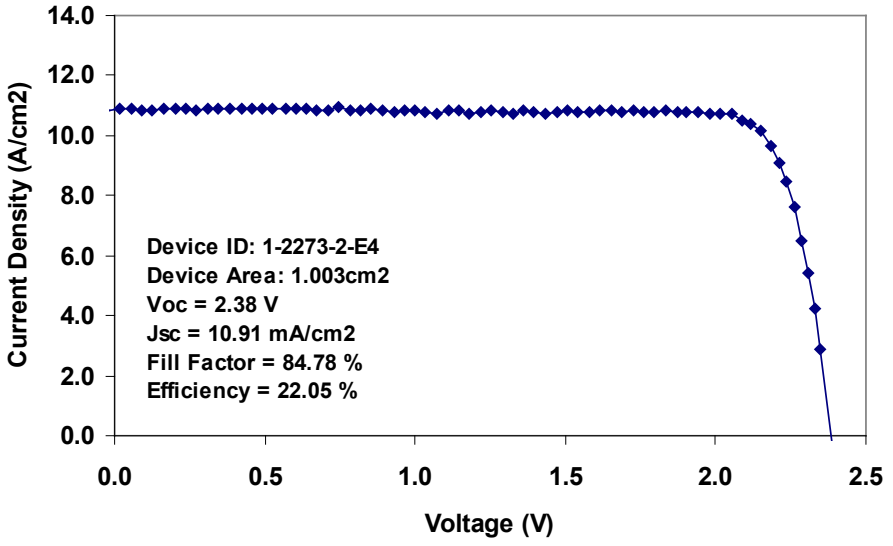

Figure 6: IV curve of 22% efficient liftoff solar cell fabricated by MicroLink for Task 2.2.

2.3 Cell Fabrication and Test Iteration 2

Milestone: Fabrication and test of solar cell.

Deliverable: Dual-junction cell with efficiency 25% under 1 sun AM1.5 illumination.

Status: Submitted on schedule.

An IV curve for a nominally 25% efficient liftoff cell is shown in Figure 7. NREL measured an efficiency of 26.1% for this device, which significantly exceeds the target value. Consistent results were obtained and the average efficiency exceeds the target value by more than 0.5%.

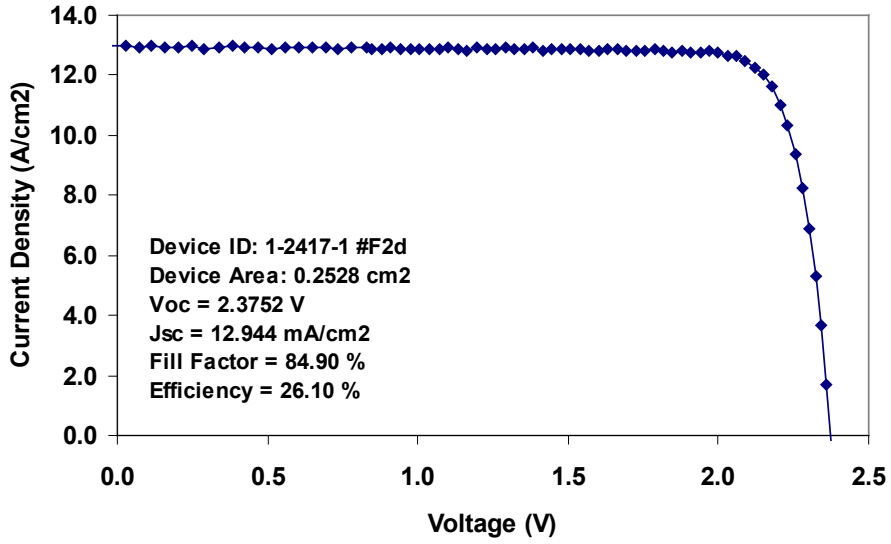

Figure 7: IV curve of 26% efficient liftoff solar cell fabricated by MicroLink for Task 2.3.

2.4 Cell Fabrication and Test Iteration 3

Milestone: Fabrication and test of solar cell.

Deliverable: Multi-junction cell with efficiency 27% under 1 sun AM1.5 illumination.

Status: Submitted on schedule.

In this task, we successfully developed a dual-junction epitaxial liftoff cell with an efficiency of 27% under AM1.5 illumination. The IV curve from a sample dual-junction cell is shown in Figure 8. In this case, the cell efficiency under AM1.5 illumination is 27.4%.

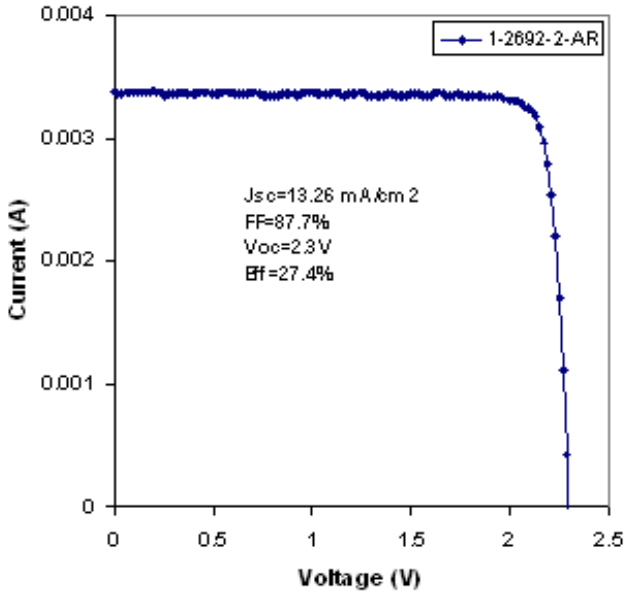

Figure 8: IV curve for a 27.4% dual-junction ELO cell under AM1.5 illumination.

In further work, MicroLink has developed a triple-junction ELO cell that has an efficiency of 30% under AM1.5 illumination as shown in Figure 9.

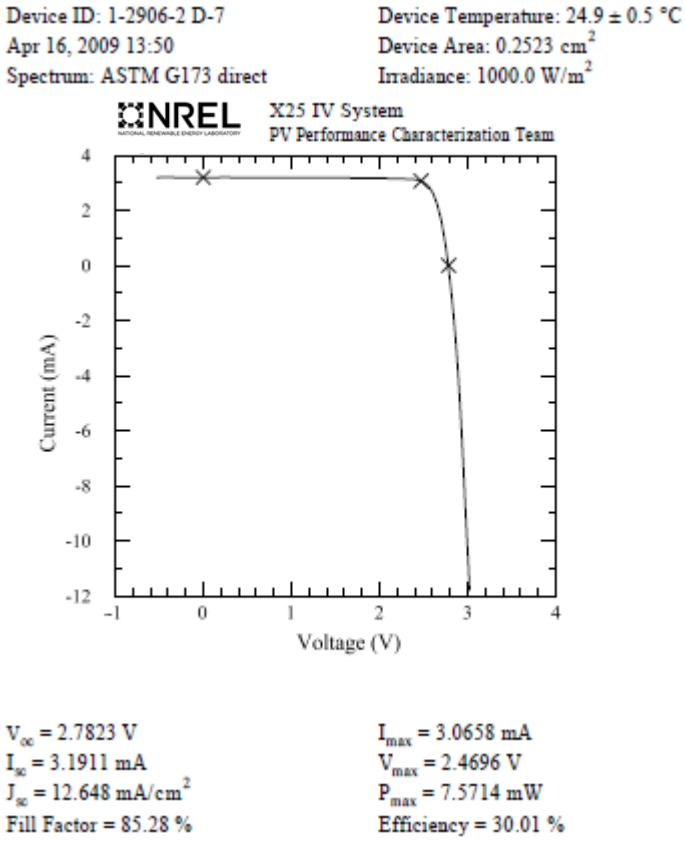

Figure 9: IV curve for a 30% efficient triple-junction ELO cell under AM1.5 illumination.

Figure 10 shows a plot of MicroLink's maximum ELO solar cell efficiency at one sun AM1.5 illumination. Note that the efficiency has increased from 10% at the start of the SAI program to the current value of 30%.

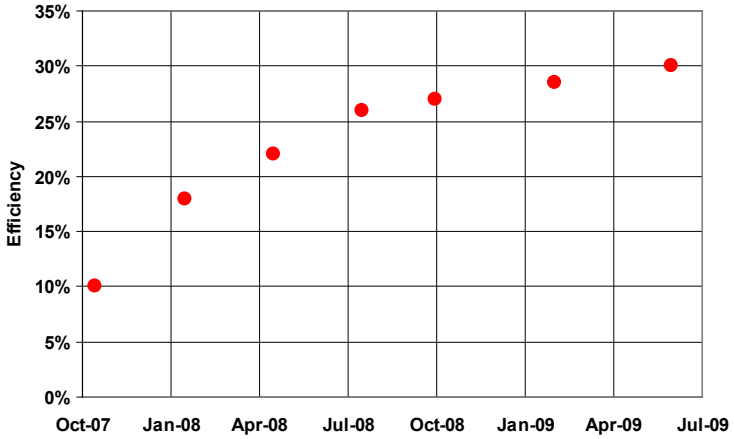

Figure 10: Increasing efficiency of dual-junction solar cells produced in MicroLink's epitaxial liftoff development program. The data points indicate average efficiencies over at least five devices.

2.5 Growth Process Development

Milestone: Solar cell junctions with good quantum efficiency (1 of 3 associated with this task)

Deliverable: Peak quantum efficiency of GaAs junction > 80%. Peak quantum efficiency of InGaP junction > 80%.

Status: Submitted on schedule.

This milestone was achieved by 1) developing and optimizing GaAs single junction solar cells, 2) developing and optimizing InGaP single junction solar cells, and 3) integration of the GaAs and InGaP cells into a single monolithically-grown dual-junction cell. Quantum efficiency spectra measured by NREL are shown in Figure 11.

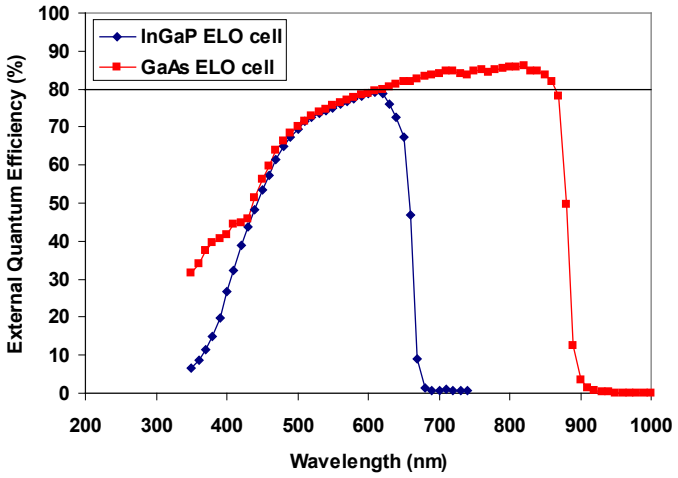

Figure 11: External quantum efficiency (EQE) for ELO GaAs (red) and InGaP (blue) single junction cells.

Milestone: Solar cells with good fill factor (2 of 3 associated with this task)

Deliverable: Fill factor of solar cell >75%.

Status: Submitted three months ahead of schedule.

The second milestone associated with this task was to obtain a fill factor in excess of 75%. This was achieved by improving ELO processing and device structure, which resulted in dramatic improvements in the efficiency and fill factor values over early devices. Cells with fill factor in excess of 85% were achieved.

Milestone: Process for fabricating liftoff solar cells (3 of 3 associated with this task).

Deliverable: Completely defined process for growing and lifting off solar cells. Liftoff of solar cell structure from 4-inch diameter wafer. Liftoff in one piece, reduction in relative cell efficiency <5% compared with cell of same design on 620 μm thick GaAs substrate.

Status: Submitted two months ahead of schedule.

The goal of this task was to develop and implement a process for fabricating dual-junction solar cell structures on 4-inch diameter wafers and lifting the solar cell structures off the wafer in one piece. Liftoff in one piece was verified by the absence of cracks or breaks in the lifted-off structure and by our ability to fabricate solar cells on more than 50% of the area of the lifted-off structure. An example of an array of lifted-off solar cells is shown in Figure 12. ELO has also been demonstrated on 6-inch diameter GaAs wafers. Efficiency measurements were made on lifted off dual-junction cells and on equivalent dual-junction cells on thick GaAs substrates.

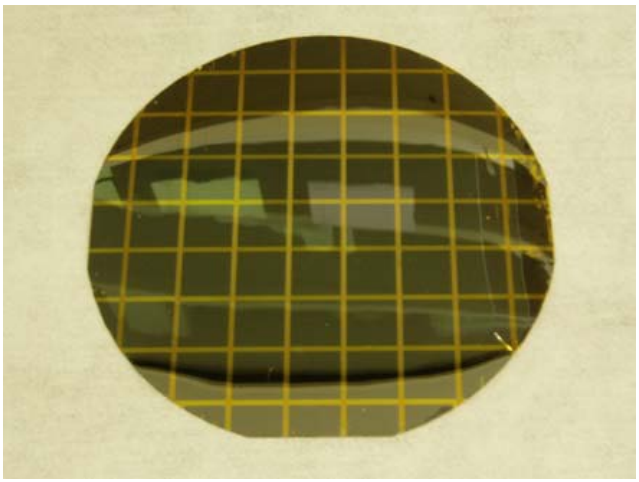

Figure 12: Array of solar cells made from one-piece lift-off from 4-inch diameter wafer.

The quality of the ELO cells is demonstrated by the fact that the relative efficiency of the ELO cells is within 5% of the efficiency of a cell of the same design on a 620 µm thick GaAs substrate. Specimen data are presented in Figure 13, from which it can be seen that that the IV curves of the (non-AR coated) ELO device and corresponding non-ELO device are almost identical. The efficiency for the ELO and non-ELO devices are, respectively, 19.6% and 19.2%. Note that the efficiency of the ELO solar cell is slightly higher than that of the non-ELO cell. Similar results were obtained from other pairs of solar cells on the two wafers.

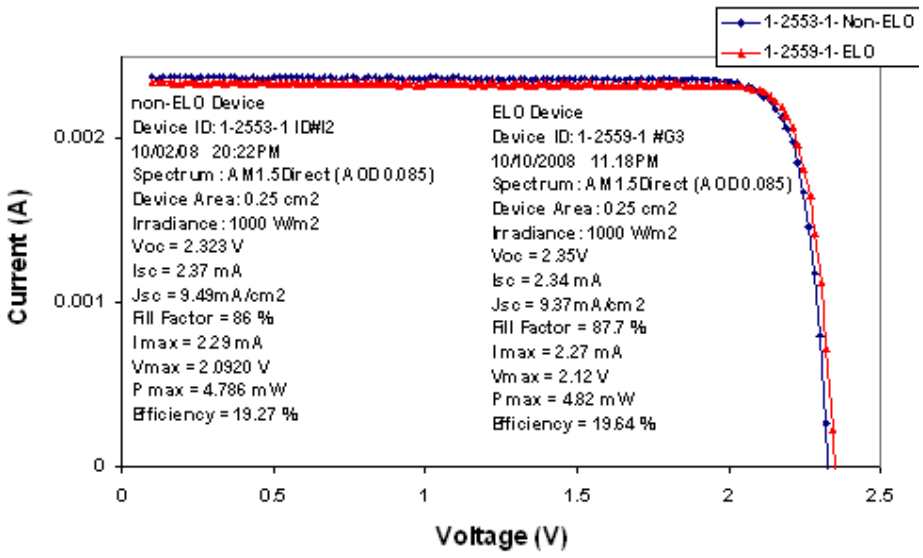

Figure 13: I-V curves from ELO and non-ELO devices.

2.6 Growth Cost Reduction: Substrate Reuse

Milestone: 1x reuse of wafer. (Milestone 1 of 3 associated with this task.)

Deliverable: Peak QE>80% in GaAs and InGaP junctions after wafer is reprocessed once.

Status: Submitted on schedule.

GaAs wafers on which dual junction solar cells had been grown, and on which the ELO process had been performed once, were subjected to a series of chemical cleaning and repolishing processes followed by epi-ready wafer preparation. Growth of dual junction solar cells was then performed in the standard manner. A control sample in the form of a new substrate was also placed in the same growth run. The dual junction solar cells grown on reworked and new substrates were then processed into ELO devices. The measured quantum efficiency curves of the resulting ELO devices are shown in Figure 14, from which it is evident that the peak quantum efficiency of both the InGaP and GaAs sub-cells is >80%.

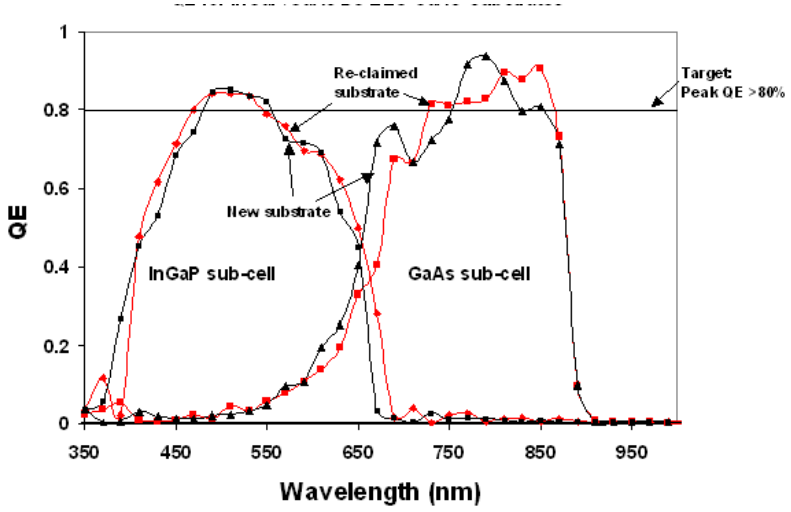

Figure 14: Quantum efficiency measurements of ELO dual junction cells grown on new and reclaimed substrates.

Milestone: 2x reuse of wafer. (Milestone 2 of 3 associated with this task.)

Deliverable: Peak quantum efficiency >80% in GaAs and InGaP junctions after wafer reprocessed twice.

Status: Submitted on schedule.

The rework procedure described above was performed on a GaAs substrate that had been used twice for solar cell growth and liftoff. Growth of dual junction solar cells was then performed in the standard manner. A control sample in the form of a new substrate was also placed in the same growth run. The dual-junction solar cells grown on reworked and new substrates were then processed into ELO devices.

Figure 14 compares the quantum efficiency vs. wavelength curves of dual junction solar cells grown on a virgin substrate, on a substrate that has been reprocessed once, and on a substrate that has been reprocessed twice. In this case, the new 100 mm-diameter GaAs substrate has a nominal thickness of 650 µm, thickness of the substrate that has been reprocessed once is approximately 600 µm, and the thickness of the substrate has been reprocessed twice is approximately 350 µm.

From Figure 14, it can be seen that the QE curves of the of the InGaP and GaAs sub cells for the new substrate, for the once-reused substrate, and for the twice-reused substrate are all similar, which suggests that the properties of the solar cell do not depend strongly on the number of times the wafer has been reused, or on the thickness of the wafer within the range 300 µm to 650 µm. The peak quantum efficiency of both the InGaP and GaAs sub-cells is >80%.

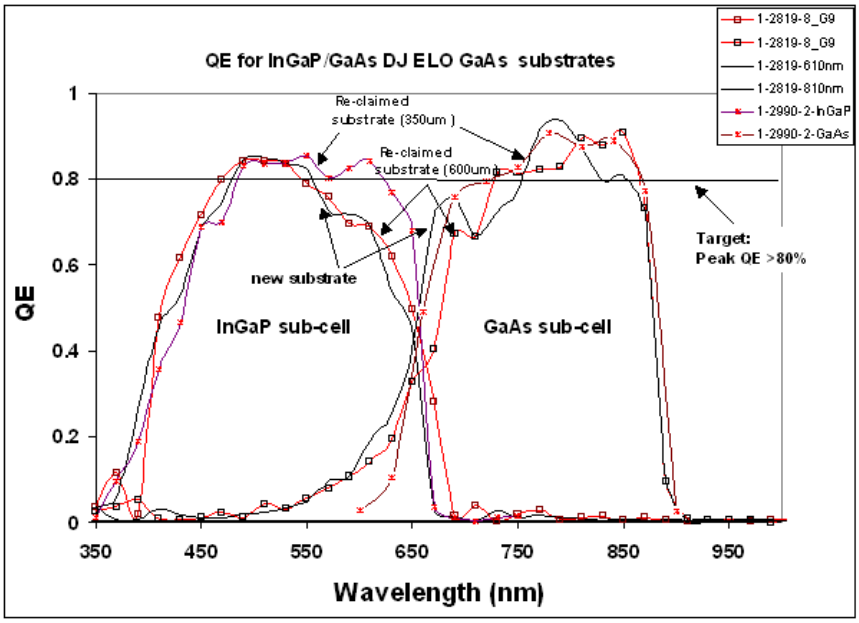

Figure 15: Quantum efficiency measurements of ELO dual junction cells grown on a virgin substrate, and on substrates that have been reprocessed once and twice.

Milestone: Process for significantly reducing cost of multi-junction solar cells. (Milestone 3 of 3 associated with this task.)

Deliverable: Cost reduction of 25% for liftoff cells grown on reused GaAs substrate. Baseline cost is standard (non-ELO) cells grown on 620 µm thick GaAs substrate.

Status: Submitted on schedule.

We developed a cost model for performing ELO and reprocessing the GaAs substrate after ELO. Inputs to the model included MicroLink's actual costs and price quotations obtained from vendors of repolishing services. Based on this information, we calculate that, by using ELO, it should be possible to reduce the cost of multi-junction solar cells by at least 25%.

2.7 InGaAs Third Cell Development

Milestone: Develop an InGaAs (E_g = 1.0 eV) single junction cell.

Deliverable: InGaAs (E_g = 1.0 eV) single junction cell with efficiency >8% (no AR coating) and fill factor >65%.

Status: Submitted on schedule.

The InGaAs solar cell was successfully grown by using metamorphic (MM) buffer layers. Fabrication of a 1.0 eV InGaAs MM solar cell is an important step towards realizing a triple junction MM solar cell. Fabricating the 1.0 eV MM solar cell involved two important developments:

1. Metamorphic buffer layer development
2. 1.0 eV InGaAs cell development

The IV curve of a sample InGaAs solar cell is shown in Figure 16. An analysis of the IV curve shows an efficiency of 9.9% and a fill factor in excess of 65%.

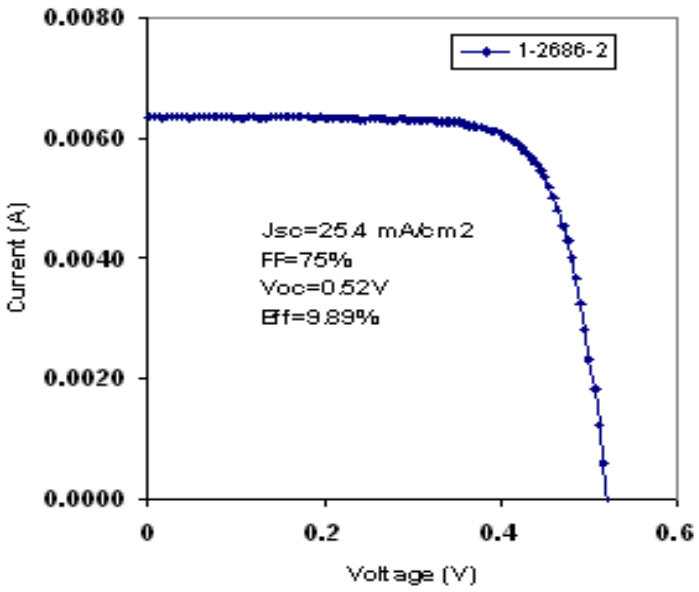

Figure 16: IV curve for a 1.0 eV InGaAs metamorphic solar cell under AM1.5 illumination.

2.8 Inverted Triple Junction Optimization

Milestone: Integration of InGaAs third junction and tunnel junction.

Deliverable: Epitaxial liftoff of complete triple junction cells from 4-inch GaAs wafers. No efficiency target.

Status: Submitted on schedule.

In this task, MicroLink has successfully developed an inverted 1 eV InGaAs solar cell and has integrated it with the dual junction cell to make an inverted triple junction cell.

The IV curves for a triple junction solar cell are shown in Figure 17. The cell shows an efficiency of 19% and Voc of 2.68 V (without AR coating).

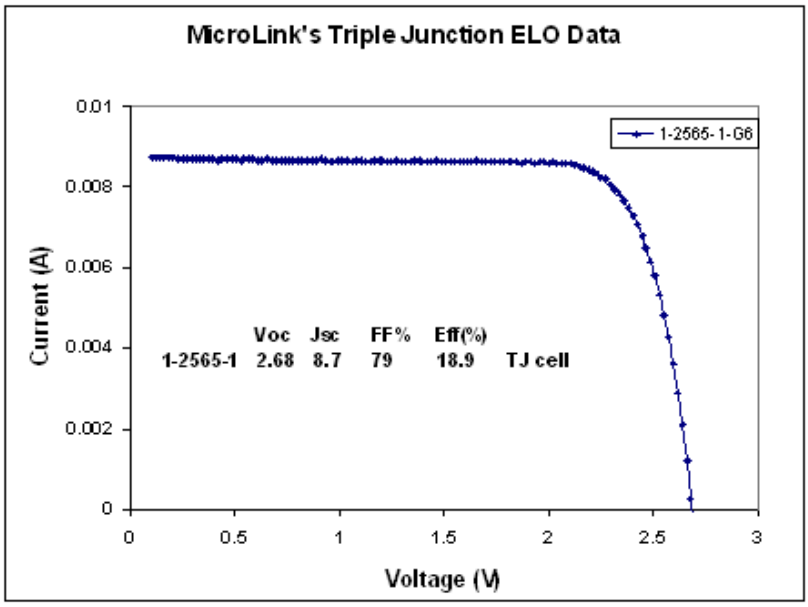

Figure 17: IV curve for triple junction ELO solar cell without AR coating.

2.9 ELO of Triple Junction Cell

Milestone: Epitaxial liftoff of triple junction IMM solar cells from full 4-inch wafer.

Deliverable: 4-inch wafer of triple junction IMM solar cells with efficiency = 27% at 1 sun, AM 1.5.

Status: Submitted on schedule.

This task was accomplished by optimizing the triple junction cell and buffer developed in Task 2.8. Performance optimization was an iterative process in which multiple structure and growth parameters were altered to incrementally improve the performance of the cell. In this work, cells with an active area of 0.2543 cm^2 were fabricated and were characterized by measuring IV curves.

Specimen results from the IV analysis of one wafer are shown in Table 2, from which it is clear that the efficiency target of 27% has been achieved. The fill factor is in excess of 86%. It should be noted that the Voc of the cells is approximately 2.77 V, which is an improvement of about 0.4 V from the Voc obtained from a dual junction ELO cell. However, given that the Voc of the single junction InGaAs cell is ~0.48 V, there is some scope for further improvements of Voc and efficiency.

Table 2: Results of IV measurements on triple junction ELO cell with AR coating from wafer 1-2906-2.

NREL- SAI Deliverable 27% +/-2% (26.46%v-27.54%)					
1-2906-2- TJ cell					
Device	Area	Voc	Jsc	FF	Efficiency
D-5	0.2543	2.771755	11.36902	86.85954	28.217823
D-7	0.2543	2.768938	11.30165	86.921	28.041936
E-5	0.2543	2.761874	11.31531	86.90401	27.998726
D-8	0.2543	2.770772	11.24366	86.77956	27.871091
D-4	0.2543	2.768866	11.28542	86.50274	27.866204
E-6	0.2543	2.75	11.31496	86.52573	27.756141

3.1 Top Metal Optimization:

Milestone: Determine optimum composition, and thickness of top metal.

Deliverable: Reduction in relative cell efficiency <5% of efficiency of dual junction cell without ELO. No absolute efficiency goals.

Status: Submitted on schedule.

This was achieved by determining how the speed of the ELO process and the quality of the resulting solar cell material depended on the composition and thickness of the top metal. One constraint on the metal was that it had to be compatible with the solution used to etch away the release layer.

3.2 Contact Grid Metal Optimization:

Milestone: Determine optimum composition, and thickness of grid metal.

Deliverable: Grid metal contact resistance within 5% of the contact resistance of a baseline non-lifted off cell.

Status: Submitted on schedule.

We investigated ohmic metal compositions. Cells with grid structures with various metal shadowing ranging from 5% to 15% were fabricated and tested on single junction GaAs and InGaP ELO wafers and non-ELO wafers. The contact grid metal was either Ti/Au or Au/GeNi/Au or in some cases only Au. The metal contacts were studied for contact resistivity and the efficiency of the single junction solar cells as a function of metal thickness. We verified that the ELO process does not alter the properties of grid metal on a single junction cell and that the same metallization schemes can be employed as on non-ELO solar cells.

3.3 QC Process Development

Milestone: Develop a quality control process for the liftoff solar cell fabrication.

Deliverable: Integrate solar cell production with MicroLink's Quicklot QC process for routine solar cell evaluation. Measure parameters such as efficiency, fill factor, Voc, and Isc.

Status: Submitted eight weeks ahead of schedule.

A Quality Control (QC) process was developed for ELO solar cells. The solar cell fabrication process was integrated with MicroLink's existing Quicklot quality control process. The measurements performed on the solar cells include IV curve measurements and QE measurements. The IV curve measurements allow the determination of efficiency, fill factor, Voc, and Isc. The successful completion of this task facilitated the rapid evaluation of solar cell material quality for production quality control and reduced the solar cell development cycle time from 7-10 days to 2 days or less. This allowed a very rapid pace of development in the SAI program.

4.1 Package Design

Milestone: None.

Deliverable: Tied to deliverable for task 4.2.

Status: No separate deliverable for this task.

MicroLink's subcontractor took the lead in the design and development of packaging for the cell. Amonix worked with MicroLink to identify and define methods for ELO solar cell packaging. Suitable materials and trial packaging processes were developed on mechanical samples.

4.2 Package Development

Milestone: Complete design and development of package for solar cells. Package some solar cells for test.

Deliverable: Packaged cells[1] available for test. These are the cells to be produced in Task 2.2. Reduction in efficiency between unpackaged and packaged cells to be <2% absolute.

Status: Submitted on schedule.

In this task, liftoff cells were singulated, attached to a ceramic substrate, and wire bonds were attached to the cells. The performance of packaged ELO cells was measured at NREL. As required by the milestone, the efficiency of the solar cell degrades by less than 0.5% when the bare solar cell die is packaged. An example of a liftoff cell mounted on a ceramic substrate is shown in Figure 18.

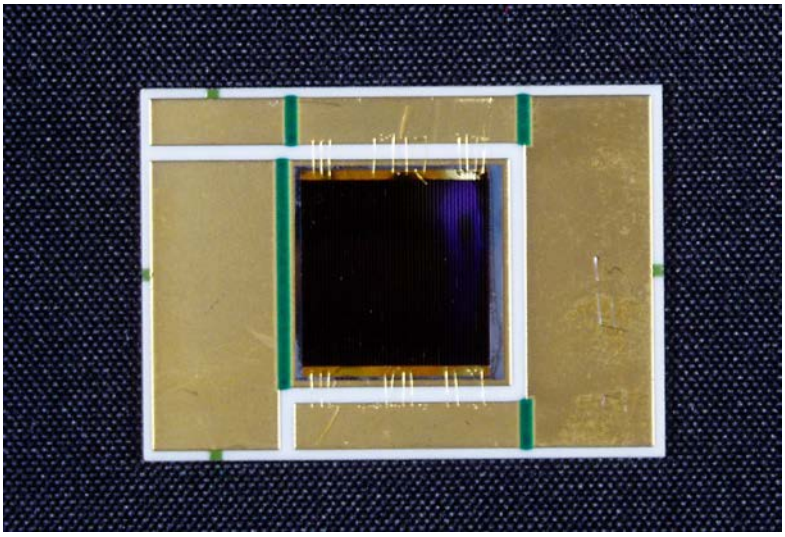

Figure 18: Example of a liftoff cell mounted on a ceramic substrate.

5.1 Integrate Packaged Cell into Concentrator

Milestone: Mount packaged cell in subcontractor concentrator.

Deliverable: Cell integrated into subcontractor concentrator system and ready for test.

Status: Submitted on schedule.

The focus of this task was to design and fabricate ELO cells of a form factor suitable for packaging into ceramic carriers that can be tested at 500 suns.

MicroLink developed a mask set to allow the fabrication of solar cells that fit into the subcontractor's concentrator. The cells have an active area of 0.58 cm^2 excluding the bus bars. The cells were designed with a 5% emitter metal shadowing. ELO cells were fabricated and tested at 1 sun at MicroLink prior to shipping to the subcontractor.

A first concentrator assembly was made based on the subcontractor's baseline die bonding procedure, which is to dispense SN62 solder paste with a syringe, pick and place the cell, and heat to re-flow, permitting the cell to float into position on the substrate. Silver mesh interconnects were hand soldered between the cell top contacts and the patterned substrate using small dots of SN62 solder paste. SN62 solder, with a melting point of ~180 ºC, is used for circuit assembly so it will remain solid during subsequent bonding of the substrate to the module baseplate with SN42 (~140 ºC Bi-Sn solder). After adding some lead wires, the first assembly was soldered onto a concentrator module base plate with SN42 solder using a hotplate. A close up view of the resulting configuration is shown in Figure 19.

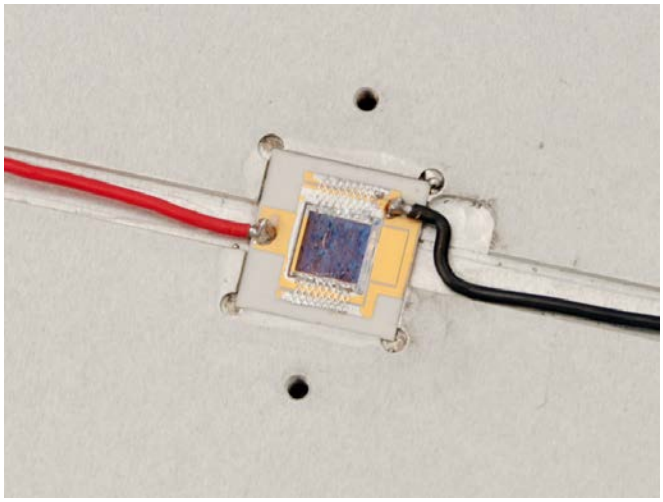

Figure 19: MicroLink ELO solar cell bonded on to concentrator module base plate.

5.2 Performance Testing in Concentrator

Milestone: Complete efficiency test of packaged triple junction cells in concentrator.

Deliverable: Efficiency of packaged triple junction liftoff cell = 25% under at least 500x concentration.

Status: Submitted on schedule.

Refer to section "Work Accomplished in Most Recent Quarter" of this report.

5.3 Reliability Testing

Milestone: Complete initial reliability testing of packaged triple junction solar cell.

Deliverable: Results of tests listed in Attachment 1 and failure analysis if necessary.

Status: Submitted on schedule.

Refer to section "Work Accomplished in Most Recent Quarter" of this report.

Conclusion

This SAI project has been a major success for MicroLink and for NREL. MicroLink has made significant technical accomplishments, which were very challenging to achieve in the required time frame. MicroLink has gained significant knowledge of the ELO process and on the sensitivity of solar cell performance to solar cell structure designs. MicroLink has demonstrated that the GaAs substrate on which the solar cell is grown can be reused at least three times, enabling significant cost reduction. The efficiency of a GaAs ELO solar cell has been increased from an initial value of 10% when the program started to 30% at the program end. Very good quantum efficiency, fill factor, and cell efficiency values have been obtained for single-junction, dual-junction, and triple-junction ELO cells. The reproducibility of the ELO process has significantly increased since the start of the program. The US Government, specifically NREL, has enabled the development of a technology that has enormous potential to reduce the LCOE for CPV electricity.

Future work on the ELO will concentrate on packaging the cells for use in terrestrial concentrators and the integration of these cells into larger arrays. This development is necessary for commercial acceptance since the ultra-thin ELO cells are unique and potential customers do not necessarily have experience with the required handling and packaging techniques. The full potential of ELO solar cells in concentrators is yet to be explored.